ORIGINAL PAPER

The structure characterization and biological activities of new polysaccharides from *Armillariella tabescens* (AT-P) and *Tricholoma portentosum* (TP-P)

Liqian Zhou[1,2] · Xiang Ding[1,2,3,4] · Yiling Hou[1]

Abstract

Polysaccharide is one of the four fundamental substances that make up life and have various important biological activities. A deep understanding of the structure and activity of polysaccharide molecules is of guiding significance for the development of polysaccharides. The structure characterization of two new polysaccharides from *Armillariella tabescens* (AT-P) and *Tricholoma portentosum* (TP-P) by HPGPC, GC-MS, NMR and FT-IR indicated that AT-P was composed of glucose and galactose in a ratio of 3:8. Its skeleton structure was consisted of (1→6)-galactose residues and (1→3,6)-galactose residues with three branched chains. The TP-P was consisted of composed of rhamnose, xylose, glucose, galactose in the ratio of 1:1:2:9. Its skeleton structure was consisted of (1→4)-galactose residues, (1→4)-glucose residues and (1→2,6)-galactose residues with one branched chain. Within the concentration range of 1.25 and 40 µg/mL, both AT-P and TP-P could enhance the proliferation ability of T cells, B cells, and RAW 264.7 cells. AT-P and TP-P could significantly ($P < 0.01$) improve the proliferation efficiency of B cells at 20 µg/mL and 10 µg/mL, respectively, with a maximum of 70.16% and 76.28%, respectively. Both AT-P and TP-P could promote the secretion of IL-1β and TNF-α by RAW 264.7 cells and promote the secretion of IL-1 by B and T cells. However, neither of they could not promote the secretion of IL-10 by RAW 264.7 cells and T cells. Their effects on the secretion of TNF-α by T and B cells were also different.

Keywords *Armillariella tabescens* · *Tricholoma portentosum* · Polysaccharide · Structure characterization · Biological activities

✉ Xiang Ding
biostart8083@126.com

✉ Yiling Hou
starthlh@126.com

1. Key Laboratory of Southwest Wildlife Resource Conservation Ministry of Education, College of Life Sciences, China West Normal University, Nanchong, Sichuan Province 637009, China

2. College of Environmental Science and Engineering, China West Normal University, Nanchong, Sichuan Province 637009, China

3. Academy of Agricultural Sciences of Dazhou City, Dazhou, Sichuan Province 635099, China

4. Xichong Xinghe Biotechnology Co., Ltd, Xichong, Sichuan Province 637299, China

Introduction

Edible fungi are a type of large fungi with dual medicinal and edible functions, which have been used as folk medicine and healthy food since ancient times. In China, there are abundant edible mushroom resources and a long history of consumption. About a quarter of the world's edible mushroom species can be found in their footprints on the land of China. *Armillariella tabescens* (Scop.ex Fr.) Sing belongs to the *Basidiomycota, Umbelliformes, Tricholomataceae*, and *Armillaria genera*, which mainly grows in tropical or subtropical areas and is distributed in Sichuan, Yunan, Guangxi province in China. Its cap is 3–8 cm wide, flattened and semi spherical, gradually flattened at the back, and blunt in the middle; the cover is not sticky, honey yellow or yellow brown; the edge of the lid is slightly upturned. The mushroom flesh is white or milky yellow in color. The stalk is 3-12 cm long and 0.3-1 cm thick, almost equally thick.

The upper part is white, and the middle part is gray brown to black brown below, often twisted. *Tricholoma portentosum* (Fr.) Quél belongs to *Basidiomycota, Umbelliformes, Tricholoma family*, and *Tricholoma genus*, which is widely distributed in Jilin, Gansu, Liaoning, Sichuan, Heilongjiang province in China. Its cap has a diameter of 5–10 (12) cm, initially hemispherical in shape, later nearly flattened, with a central protrusion and a nearly smooth surface with radiating dark stripes. The mushroom flesh is white, with a yellowish color in the later stage, slightly thin, and no obvious odor. The stalk is nearly cylindrical, rod-shaped, slightly thick, 3.5-10 cm long, 0.5-1.6 cm thick, white, and appears as yellow brown patches in the lower part.

Polysaccharides from edible fungi and medicinal fungi are important components of endogenous bio-active molecules, and also involved in the cytoskeleton formation. In the past 20 years, research reports on the polysaccharides biological activities of edible and medicinal fungi have mainly focused on immune regulation, antiviral, antioxidant and hypoglycemic aspects, and their effects are multi-channel, multi-link and multi-target [1–4]. Immune experiments have proved that polysaccharides from edible and medicinal fungi could not only activate natural killer cells (NK), B cells and T cells, but also promote the production of cytokines, activate complement and play a multifaceted regulatory role on the immune system [5, 6]. However, the complexity and diversity of polysaccharides pose significant challenges to the structural determination and characterization of polysaccharides, as well as the molecular mechanisms underlying their biological activities. Due to the difficulty in separating and purifying polysaccharides from edible and medicinal fungi, as well as the complexity of their own structures, there are not many studies that can purify homogeneous polysaccharides and elucidate their structures. Moreover, most studies on the immunomodulatory activity of polysaccharides from edible and medicinal fungi have focused on the biological activity of their crude extracts, and it is not clear which components or main components play a role in their mixtures or complexes, greatly restricting the application of active polysaccharides from edible and medicinal fungi [7–9]. At present, the structure and activities of *Armillariella tabescens* and *Tricholoma portentosum* polysaccharides from Maerkang County have not been reported. In this study, two new polysaccharides AT-P and TP-P were extracted from *Armillariella tabescens* and *Tricholoma portentosum*, respectively, and the structure and activities of AT-P and TP-P were also studied to provide a data foundation for the further application of polysaccharide.

Materials and methods

Polysaccharide extraction and purification

The *Armillariella tabescens* (fresh fruiting body was 3 kg, No. AT-1) and *Tricholoma portentosum* (fresh fruiting body was 3 kg, No. TP-1) were collected in Maerkang County, Sichuan Province, China. Collect the fresh fruiting body of fungus and observe the characteristics of its cap, cover, edge, and stalk. Refer to Mao Xiaolan's 'Large Fungi in China' for morphological comparison and identification of the strains. The Identified fungus was preserved in the Key Laboratory of Southwest Wildlife Resource Conservation Ministry of Education, College of Life Sciences, China West Normal University. Grind the completely dried fruiting body (300 g for each mushroom) into powder using a high-speed grinder, add distilled water in a 1:3 ratio of material to liquid, soak at 100℃ for 6 h, centrifuge at 8000 rpm for 30 min, collect the supernatant and concentrate it to 200 mL, add anhydrous ethanol in a 1:4 ratio for alcohol precipitation, and collect the flocculent precipitate [10]. The Sevag method was used to remove proteins from crude polysaccharides. The activated DEAE-52 cellulose was packed in columns and eluted with different concentrations of NaCl (0, 0.05, 0.1, 0.2, 0.3, 0.4 mol/L NaCl) as eluent. The elution flow rate was 5 mL/min, and the amount collected in each tube was 5 mL. 50 samples were collected in each elution section. Detect the polysaccharide content in each tube using the sulfuric acid phenol method and draw the elution curve. Collect the elution peak with the highest OD value, concentrate the elution to 5–7 mL, dialyze in a dialysis bag with a capacity of 7000 Da, centrifuge, and lyophilized to obtain pure polysaccharides, which were named AT-P and TP-P, respectively.

Polysaccharide structure characterization

Fourier transform infrared spectrometer (Nicolet 5700, Thermo Scientific) was used within the wavenumber range of 4000 cm^{-1} to 400 cm^{-1} to get the FT-IR data [11]. The molecular weight was tested via HPGPC [12]. High-performance liquid chromatography (HPLC) was used for the analysis of the monosaccharide composition of polysaccharides. HPLC determination conditions: zorbax Carbohydrate Analysis col (4.6 mm x 250 mm) chromatography column; 75% acetonitrile as mobile phase; RID detector; constant column temperature of 30℃; RID detector temperature of 35℃; flow rate of 1.4 mL/min; injection volume 10 μL; keep for 15 min [13]. The methylation-derivatized polysaccharide product was determined by GC-MS (Agilent 7890 A, USA). The measurement conditions are as follows: the chromatographic column is an HP-5ms column (30 m x 0.25 mm x 0.25 μm). The carrier gas is high-purity helium

with; an injection volume of 5µL; and an injection port temperature of 250℃. The heating program starts at an initial temperature of 80 ℃, maintains it for 3 min, and then rises to 200℃ at a rate of 10℃/min for 10 min [14]. The NMR spectra were determined by the Varian Unity INOVA 400/45 (Varian Medical Systems, USA) using tetramethylsilane (TMS) as the internal reference. MestReNova 9.0 software was used to analyze data [15].

Effects of polysaccharide on T cells, B cells and RAW264.7 cells

The proliferation effects of polysaccharides on cells were determined via CCK-8 method [16]. The experimental setup includes experiment groups (AT-P, TP-P), blank groups (Control), and positive control groups (LPS), with 6 replicates in each group. Dilute cells of the logarithmic phase of growth to 1×10^5 cells/mL. 100µL/well cells were added to a 96-well plate and incubated in a constant temperature incubator at 37 ℃ and 5% CO_2 for 24 h. Different concentrations of polysaccharide solution were added and incubated with CCK-8 solution at constant temperature for 3 h, the absorbance value was measured at a wavelength of 450 nm using an enzyme-linked immunosorbent assay (ELISA) reader, and the cell morphology was observed under a microscope. The cytokines was detected by the ELISA kit (Wuhan BOSTER Biological Technology Co., Ltd.; Wuhan) [17].

Statistical analysis

All statistical comparisons were analyzed using a one-way analysis of variance (ANOVA) test followed by Student-Newman-Keuls test. *: $P < 0.05$; **: $P < 0.01$.

Results and discussion

The molecular weight of AT-P and TP-P

There were both four main elution peaks, respectively, with the NaCl concentration increased. The neutral polysaccharides in distilled water and 0.05 mol/L NaCl solution were collected, respectively, as the subject of research. The yield of AT-P and TP-P in the total fruiting body were 0.2% and 0.3%, respectively (Fig. 1A and B). The weight-average molecular weight (Mw) of AT-P and TP-P were 17 600 Da and 19 101 Da, respectively (Fig. 1C and D). Polysaccharides, as biological macromolecules, have variable molecular weights ranging from ten to one million [18]. The molecular weight of polysaccharides has a significant impact on their biological activity. Their ability to penetrate

cell membranes is poor if the molecular weight of polysaccharides is too high with their water solubility is low, which is not conducive to their biological activity. However, they will have no biological activity if the molecular weight of polysaccharides is too small. Polysaccharides with molecular weight ranging from 10,000 to 50,000 Da exhibit strong biological activity [19]. In this study, the molecular weights of both polysaccharides were within the biologically active range (10,000 to 50,000 Da), indicating their certain biological activity.

FT-IR analysis of AT-P and TP-P

In the IR spectrum of AT-P (Fig. 1E), the O-H stretching vibration peak was the broad peak at 3425.88 cm^{-1} [20], the -CH$_2$ peak was at 2928.49 cm^{-1}, the C＝O peak was at 1632. 92 cm^{-1}, the C-H peak of - CHO was at 1404.47 cm^{-1}, the C-O peak was at 1077.59 cm^{-1} [21].

In the IR spectrum of TP-P (Fig. 1F), the O-H stretching vibration peak was at 3440.18 cm^{-1}, the -CH$_2$ peak was at 2922.48 cm^{-1}, the C＝O peak was at 1638. 92 cm^{-1}, the C-H peak of - CHO was at 1406.91 cm^{-1}, the C-O peak was at 1079.91 cm^{-1}, and the C-H rocking vibration peak was at 616.45 cm^{-1}. There was no signal near 1730 cm-1 in both FT-IR spectrum of AT-P and TP-P, indicating that these two polysaccharides didn't contain uronic acid [22]. Infrared spectroscopy is a process in which molecules selectively absorb certain wavelengths of infrared radiation, causing transitions between vibrational and rotational energy levels in the molecule, thereby obtaining information on the chemical bonds or functional groups present in the molecule. IR spectroscopy is one of the standard techniques that was used for characterization of polysaccharides, such as carrageenans, pectins and alginates, in which the different structural elements are assigned to different absorption bands [22]. In this study, both AT-P and TP-P polysaccharides showed characteristic absorption peaks and fingerprint absorption peaks, with no impurity peaks such as amino acids, indicating high purity of the extracted polysaccharides.

Monosaccharide composition results of AT-P and TP-P

The peaks of monosaccharide composition of AT-P with retention time of 7.934 and 8.486 min were glucose (Glc) and galactose (Gal), respectively. The ratio of Glc: Gal was about 3:8 (Fig. 1G). The peaks in TP-P experiments with retention time of 4.946 min, 5.716 min, 7.771 and 8.437 min were Rhamnose (Rha), Xylose (Xyl), Glucose (Glc) and galactose (Gal), respectively. The ratio of Rha: Xyl: Glc: Gal was about 1: 1: 2: 9 (Fig. 1H). Two types of polysaccharides were extracted and purified from *Armillariella tabescens*, a
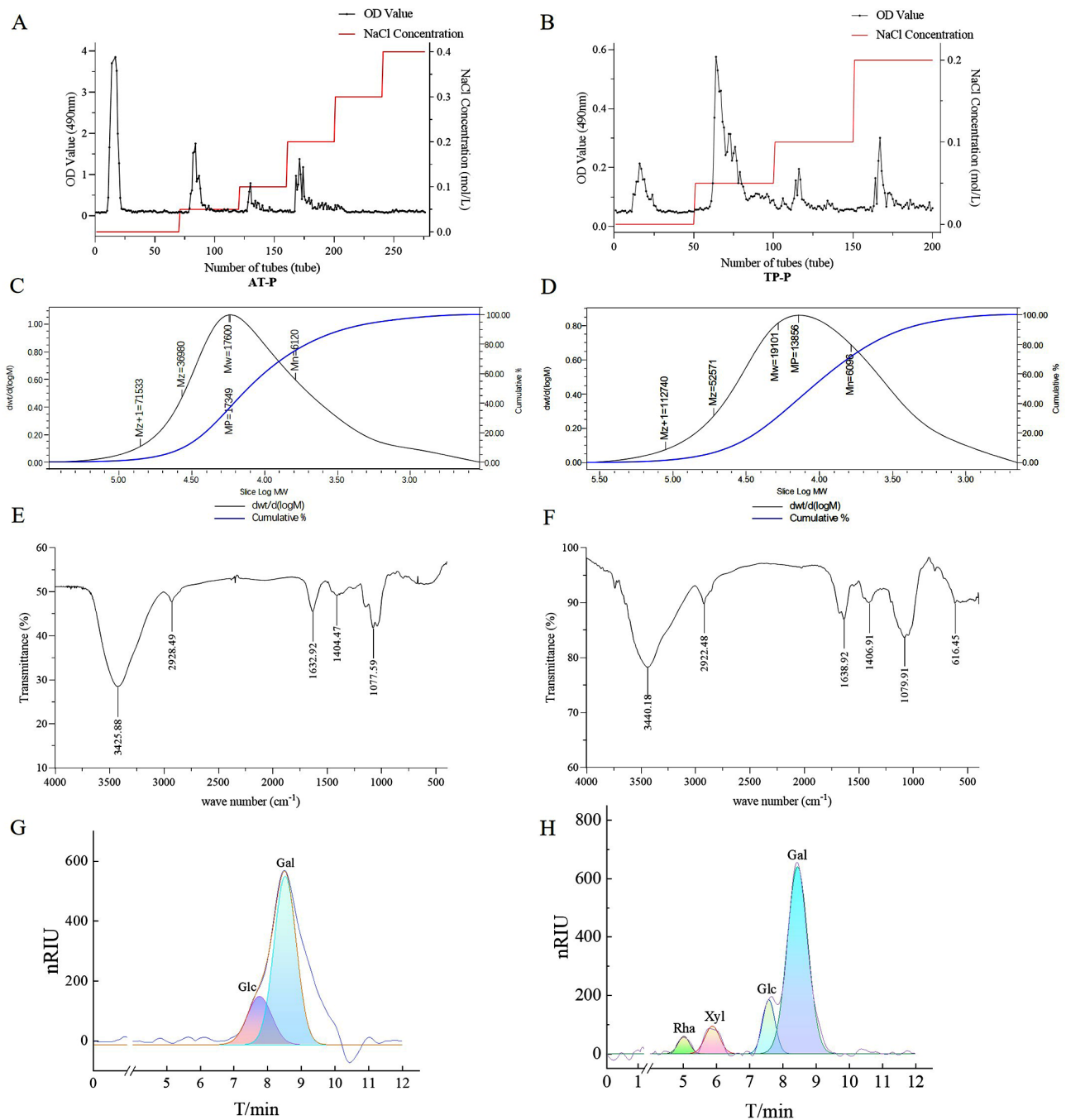
Fig. 1 (**A**) Elution curve of AT-P by column chromatography. (**B**) Elution curve of TP-P by column chromatography. (**C**) The molecular weight of AT-P. (**D**) The molecular weight of TP-P. (**E**) The fourier transform infrared spectra of AT-P. (**F**) The fourier transform infrared spectra of TP-P

water-soluble polysaccharide AT-HW composed of (1→6) - linked D-pyranose and D-galactose; and a water insoluble polysaccharide AT-AL composed of (1→3)-α-D-gluctose, and it was found that AT-HW could affect macrophages and T cells to participate in immunity, while AT-AL mainly activates macrophages to produce SOA and activates lysosomal enzymes, thereby mediating immune regulatory mechanisms and achieving anti-tumor effects [23]. A

polysaccharide TS-P with (1–4) - Arap, (1–4,6) - D-Manp, and two (1–6) - Galp as the main chains was extracted and purified from the *Tricholoma portentosum* collected in Yajiang County, Ganzi Prefecture, Sichuan Province. The polysaccharide TS-P was confirmed to have anti-tumor potential and could significantly ($P < 0.05$) promote the proliferation of B cells, T cells, macrophages, and secretion of cytokines [24]. In this study, the polysaccharide AT-P was composed

Table 1 GC-MS results of methylation analysis of *Armillariella tabescens* polysaccharide (AT-P)

No	Molecular Ion Fragments	Linkage	m/z
1,6-Glcp (A)	2,3,4-tris-O-methyl-1,6-di-O- trimethylsilyl-Glcp	1,6-	71 73 75 88 89 101 116 131 133 146 341 590
1-Galp (B)	2,6-di-O-methyl-1,3,4-tris-O-trimethylsilyl-Galp	1,3,4-	73 75 89 116 131 133 146 147 159 191 303 595
1,6-Galp (C)	4,6- di-O-methyl-1,2,6-tris-O-trimethylsilyl-Galp	1,6-	71 73 75 88 101 131 133 146 147 159 281 400 502
1,3,6-Galp (D)	2,4- di-O-methyl-1,3,6-tris-O-trimethylsilyl-Galp	1,3,6-	59 73 75 89 116 131 146 147 159 191 287 421
4-Glcp (E)	1,2,3,6-tetrakis-O-trimethylsilyl-Glcp	4-	71 73 75 88 89 101 116 131 133 159 174

Table 2 GC-MS results of methylation analysis of *Tricholoma portentosum* polysaccharide (TP-P)

No	Molecular Ion Fragments	Linkage	m/z
1,4-Galp (D)	6-O-methyl-1,2,3,4-tet-O-trimethylsilyl-Glcp	1,4-	45 59 73 89 103 117 147 159 191 204 217 231 265 291 305 377 393
1,2,6-Galp (E)	3,4-di-O-methyl-1,2,6-tris-O-trimethylsilyl-Galp	1,2,6-	41 59 73 89 103 117 133 146 159 173 189 205 217 231 277 345 377
1,4-Glcp (B)	galp-1) → (4-O-1,2,3,6-tet-O-trimethylsilyl-Glcp	1,4-	69 73 103 117 147 157 191 204 217 231 271 291 305 319 361
1-Xylp (A)/1,3-Rhap (C)	xylp-1) → (3-rhap-1) → (2-O-1,6-galp	1-、1,3-	81 101 115 143 159 175 191 201 219 247 423 539 643

of glucose (Glc) and galactose (Gal), and TP-P was composed of Rhamnose (Rha), Xylose (Xyl), Glucose (Glc) and galactose (Gal), which had difference in monosaccharide composition compared to previous reports. Rhamnose (Rha), Xylose (Xyl), Glucose (Glc) were first discovered to exist in *Tricholoma portentosum* polysaccharide.

GC-MS analysis of AT-P and TP-P

The GC-MS results, consistent with the results of HPLC, indicated that AT-P was consisted of two kinds of monosaccharides: Glc and Gal, with the ratio of Glc: Gal was 3:8. The glucose residues was 2,3,4-tris-O-methyl-1,6-di-O-trimethylsilyl-Glcp and 1,2,3,6-tetrakis-O-methyl-4-O-trimethylsilyl-Glcp, which indicating glucose residues was 1,6-linked and 4-linked in AT-P. The galactose residues was 2,4-di-O-methyl-1,3,6-tris-O-trimethylsilyl-Galp, 2,6-di-O-methyl-1,3,4-tris-O-trimethylsilyl-Galp and 3,4-di-O-methyl-1,2,6-tris-O-trimethylsilyl-Galp, which indicating galactose residues was 1,3,6-linked, 1,3,4-linked and 1,2,6-linked in AT-P [25]. Considering incomplete methylation caused by the steric hindrance of C2 and C3 on the monosaccharide ring, it indicated that galactose residues was 1-linked, 1,6-linked and 1,3,6-linked in AT-P [26] (Table 1).

The GC-MS results, consistent with the results of HPLC, indicated that TP-P was consisted of four kind of

monosaccharides: Rha, Xyl, Glc and Gal, with the ratio of 1: 1: 2: 9, The GC-MS results of TP-P showed glucose residue was 6-O-methyl-1,2,3,4-tet-O-trimethylsilyl-Glcp, and galactose residues was 6-deoxy-1,2,3,4-tetrakis-O-trimethylsilyl-Galp. Considering incomplete methylation caused by the steric hindrance of C2 and C3 on the monosaccharide ring, it indicated that glucose residues and galactose residues both were 1,4-linked in AT-P. In addition, it was shown that rhamnose connects 2-O-(1,6-galactose residues) and 1-O-xylose using 1,3-O linkage as a bridge, while galactose residues have 3,4-di-O-methyl-1,2,6-tris-O-trimethylsilyl-Galp. All these results indicating that glucose residues was 1,4-linked, rhamnose residues was 1,3-linked, xylose residues was 1-linked, and galactose residues was 1,2,6-linked and 1,4-linked in TP-P [27] (Table 2). Most of the polysaccharides with outstanding biological activity are connected by (1–3) or (1–4) glycosidic bonds, which is conducive to the formation of a three strand helical stereoconfiguration and shows high biological activity. If the skeleton structure is mainly connected by (1→6) bonds or other bonds, the biological activity is lower [28]. *Lentinus edodes* polysaccharides and *Polyporus umbellatus* polysaccharides both belong to the category containing -D-glucose residue linked by (1→3) bond as the backbone of glucan exhibits strong biological activity. *Coriolus versicolor* polysaccharide, which has inhibitory effects on the growth of various tumor cells β- (1–4)-D-glucose as the main chain

Table 3 Chemical shifts of hydrogen and carbon atoms in *Armillariella tabescens* polysaccharide (AT-P)

Glycosyl residues	Chemical shifts (ppm)					
	H1	H2	H3	H4	H5	H6
1,6-Glcp (A)	5.24	3.53	3.83	3.65	3.78	3.57
1-Galp (B)	5.01	3.81	3.96	3.66	3.80	3.53
1,6-Galp (C)	4.94	3.66	4.00	3.82	4.08	3.96
1,3,6-Galp (D)	4.86	3.71	3.93	3.54	3.75	3.69
4-Glcp (E)	4.38	3.18	3.34	3.26	3.41	3.30
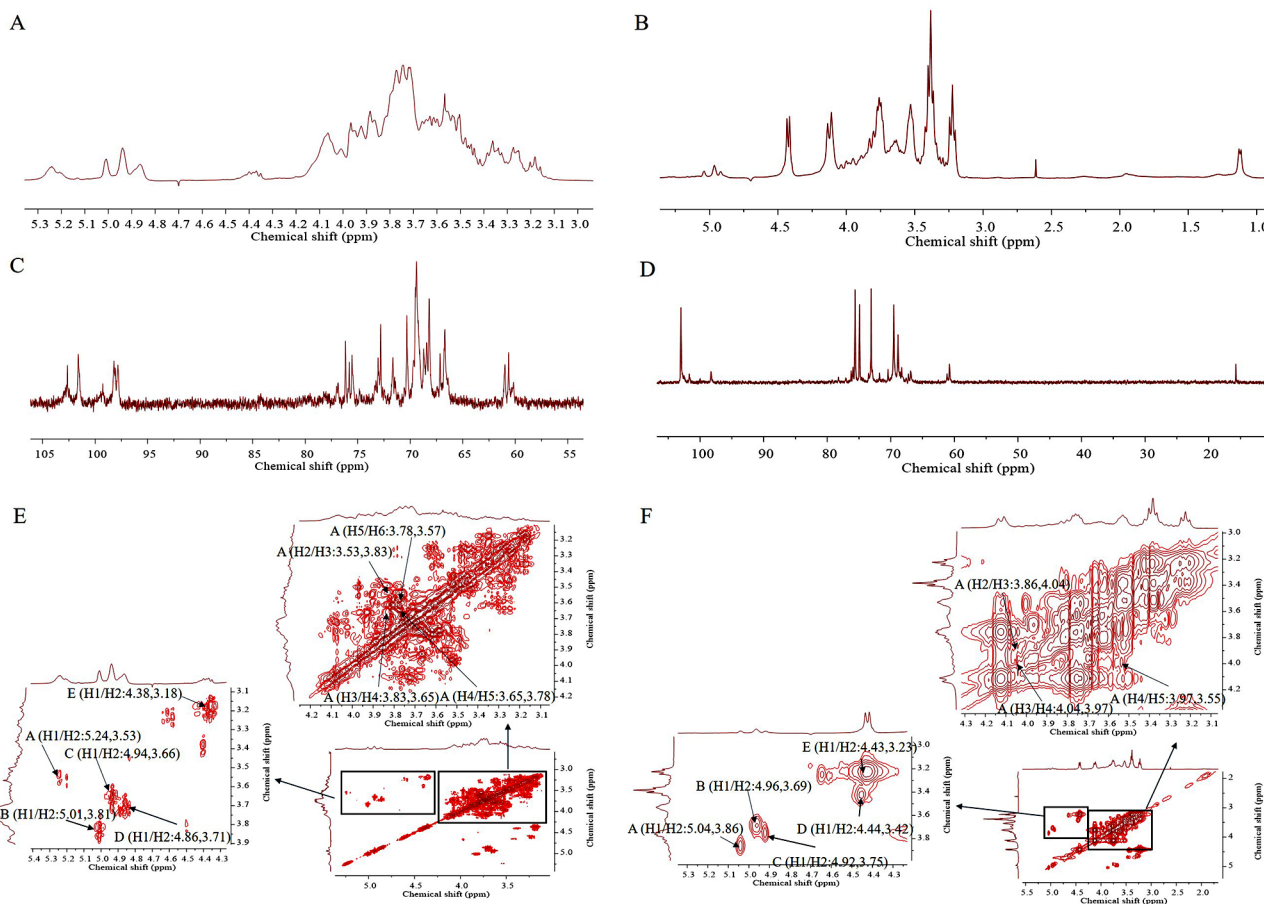
Fig. 2 **(A)** The ^{1}H NMR spectra of AT-P. **(B)** The ^{1}H NMR spectra of TP-P. **(C)** The ^{13}C NMR spectra of AT-P. **(D)** The ^{13}C NMR spectra of TP-P. **(E)** ^{1}H-^{1}H COSY spectrum of AT-P. **(F)** ^{1}H-^{1}H COSY spectrum of TP-P

[29]. However, this situation only applies to polysaccharides with a glucan skeleton. In this study, polysaccharide AT-P has a skeleton composed with (1→6)-galactose residues and (1→3,6)-galactose residues, while TP-P has a skeleton composed with (1→4)-galactose residues, (1→4)-glucose residues and (1→2,6)-galactose, which indicating that the activities of the two polysaccharides will not be consistent with previous reports.

NMR analysis of AT-P and TP-P

Nuclear magnetic resonance spectroscopy (NMR) is a powerful tool for analyzing the exact structure of how functional groups within molecules are connected [30]. ^{1}H-NMR spectra showed AT-P had five anomeric protons signals which were at δ 5.24, δ 5.01, δ 4.94, δ 4.86 and δ 4.38, respectively, that belong to 1,6-Glcp (A), 1-Galp (B), 1,6-Galp (C), 1,3,6-Galp (D) and 4-Glcp (E), respectively [31]. The hydrogen signals of H2-H6 in monosaccharides overlapped between δ 3.09 and δ 4.50 [15](Table 3; Fig. 2A). ^{1}H-NMR spectra of TP-P showed it had five anomeric protons signals, which were at δ 5.04, δ 4.96, δ 4.922, δ 4.43 and δ 4.42, respectively [32]. The comparison of the signal at δ 4.43, δ 4.42 between the ^{1}H-NMR spectra and HMQC spectra indicated that it was a split peak signal and should be the one signal peak at δ 4.43, indicating that polysaccharide TP-P only had

four anomeric protons signals. Anomeric protons signals at δ 5.04, δ 4.96, δ 4.922 and δ 4.43 belong to 1-Xylp (A), (1→4)-Glcp (B), (1→3)-Rhap (C), (1→4)-Galp (D) and (1→2,6)-Galp (E), respectively. The hydrogen signals of H2-H6 in monosaccharides overlapped between δ 3.0 and δ 4.3 [32, 33] (Table 4; Fig. 2B).

^{13}C-NMR spectra of AT-P showed that AT-P had five anomeric carbon signals at δ 102.64, δ 101.61, δ 99.27, δ 98.21 and δ 97.83, which belong to anomeric carbon signals of 1,3,6-Galp (D), 1-Galp (B), 1,6-Glcp (A), 4-Glcp (E) and 1,6-Galp (C), respectively [34]. The signals of C2-C6 in monosaccharide residues appeared between δ 55 and 80 [35] (Table 3; Fig. 2C). ^{13}C-NMR spectra of TP-P showed that TP-P had four anomeric carbon signals at δ 101.67, δ 98.25 and δ 97.85, which belong to anomeric carbon signals of (1→2,6)-Galp (D), (1→4)-Glcp (B), 1-Xylp (A) and (1→3)-Arap (C), respectively [35] (Table 4; Fig. 2D).

^{1}H-^{1}H COSY is mainly a technique for determining the coupling relationship between adjacent hydrogen in molecules [36]. The ^{1}H-^{1}H COSY spectrum of AT-P showed the signal A (H1/H2:δ 5.24/3.53), B (H1/H2:δ 5.01/3.81), C (H1/H2:δ 4.94/3.66), D (H1/H2:δ 4.86/3.71) and E (H1/H2:δ 4.38/3.18) belong to the resonant coupling signal between H-1 and H-2 of the 1,6-Glcp (A), 1-Galp (B), 1,6-Galp (C), 1,3,6-Galp (D) and 4-Glcp (E) groups, respectively [37]. According to the resonant coupling signal between adjacent hydrogen in molecules, the signals of H2-H6 of the A group are δ 3.53, δ 3.83, δ 3.65, δ 3.78 and δ 3.57, respectively [38]. The ^{1}H signals of B-E groups were also deduced (Fig. 2E). The ^{1}H-^{1}H COSY spectrum of TP-P showed that signal A (H1/H2:δ 5.04/3.86), B (H1/H2:δ 4.96/3.69), C (H1/H2:δ 4.92/3.75) and D (H1/H2:δ 4.43/3.23) belong to the resonant coupling signal between H-1 and H-2 of the 1-Xylp (A), (1→4)-Glcp (B), (1→3)-Rhap (C) and (1→2,6)-Galp (D) groups, respectively. The signals of H2-H6 of the A group are δ 3.86, δ 4.04, δ 3.97, δ 3.55 and δ 3.72, respectively [38] (Fig. 2F).

HMQC spectrum reflects the direct correlation between hydrogen and carbon signals, from which the correlation between ^{1}H and ^{13}C could be obtained [39]. HMQC spectrum of AT-P showed that signal A (H1/C1:δ 5.24/99.27), B (H1/C1:δ 5.01/98.21), C (H1/C1:δ 4.94/101.61), D (H1/C1:δ 4.86/97.83) and E (H1/C1:δ 4.38/102.64) belong to the resonant coupling signal between C-1 and H-1 of the

1,6-Glcp (A), 1-Galp (B), 1,6-Galp (C), 1,3,6-Galp (D) and 4-Glcp (E) groups, respectively [40]. According to the resonant coupling signal between directly connected ^{1}H and ^{13}C, the signals of C2-C6 in (1→4,6)-Glcp (A) group are δ 74.27, δ 72.82, δ 77.05, δ 69.48 and δ 66.61, respectively [41] (Fig. 3A). HMQC spectrum of TP-P showed that signal A (H1/C2:δ 5.04/98.30), B (H1/C2:δ 4.96/101.69), C (H1/C2:δ 4.92/98.23) and D (H1/C2:δ 4.43/103.01) belong to the resonant coupling signal between H-1 and C-1 of 1-Xylp (A), (1→4)-Glcp (B), (1→3)-Rhap (C) and (1→2,6)-Galp (D) groups, respectively. According to the resonant coupling signal between directly connected ^{1}H and ^{13}C, the signals of C2-C6 in (A) (1→4,6)-D-Manp group are δ 60.53, δ 75.91, δ 71.75, δ 76.21 and δ 68.83, respectively [40, 41] (Fig. 3B).

HMBC provides a hydrocarbon relationship for remote coupling [42]. The HMBC spectrum of AT-P showed the signals (H2/C3:δ 3.53/77.05) belonging to the resonance signal between H-2 and C-3 of 1,6-Glcp (A). The signal (H3/C4:δ 3.96/68.33) belong to the resonance signal between H-3 and C-4 of 1-Galp (B), the signal (H1/C4:δ 4.86/66.55), (H4/C5:δ 3.54/71.77) and (H5/C6:δ 3.75/68.19) belong to the resonance signal between H1 and C4, H4 and C5, H5 and C6 of 1,3,6-Galp (D), respectively [43]. The signal (H2/C1:δ 3.18/102.64) belong to the resonance signal between H-2 and C-1 of 4-Glcp (E) [44] (Fig. 3C). The HMBC spectrum of TP-P showed that the signal (H5/C3:δ 3.55/75.91) belong to the resonance signal between H-5 and C-3 of 1-Xylp (A). The signal (H4/C6:δ 3.53/69.41) belong to the resonance signal between H-4 and C-6 of 1,4-Glcp (B), and the signal (H1/C5:δ 3.44/73.48) and (H4/C3:δ 3.27/75.81) belong to the resonance signal between H1 and C5, H4 and C3 of (1→4)-Galp (D), respectively. The signal (H1/C3:δ 4.43/68.76), (H4/C2:δ 3.39/69.45), (H4/C5:δ 3.39/74.99), (H6/C4:δ 3.22/75.51) and (H6/C1:δ 3.22/103.01) belong to the resonance signal between H1 and C3, H4 and C2, H4 and C5, H6 and C4, H6 and C1 of (1→2,6)-Galp (E) [44] (Fig. 3D).

All the results above showed that AT-P was composed of Glucose and Galactose in the ratio of 3:8, and its skeleton structure was based on (1→6)-galactose residues, (1→3,6)-galactose residues, and the branch chain were composed of (1→6)- Glucose residues, →4)-glucose residues and →1)-galactose (Fig. 3E). The TP-P was composed

Table 4 Chemical shifts of hydrogen and carbon atoms in *Tricholoma portrntosum* polysaccharide (TP-P)

Glycosyl residues	Chemical shifts (ppm)					
	H1	H2	H3	H4	H5	H6
1-Xylp (A)	5.04	3.86	4.04	3.97	3.55	-
1,4-Glcp (B)	4.96	3.69	3.7	3.83	3.63	3.75
1,3-Rhap (C)	4.92	3.75	4.11	3.53	3.76	1.13
1,4-Galp (D)	4.44	3.42	3.65	3.27	3.48	3.21
1,2,6-Galp (E)	4.43	3.23	3.61	3.39	3.52	3.22
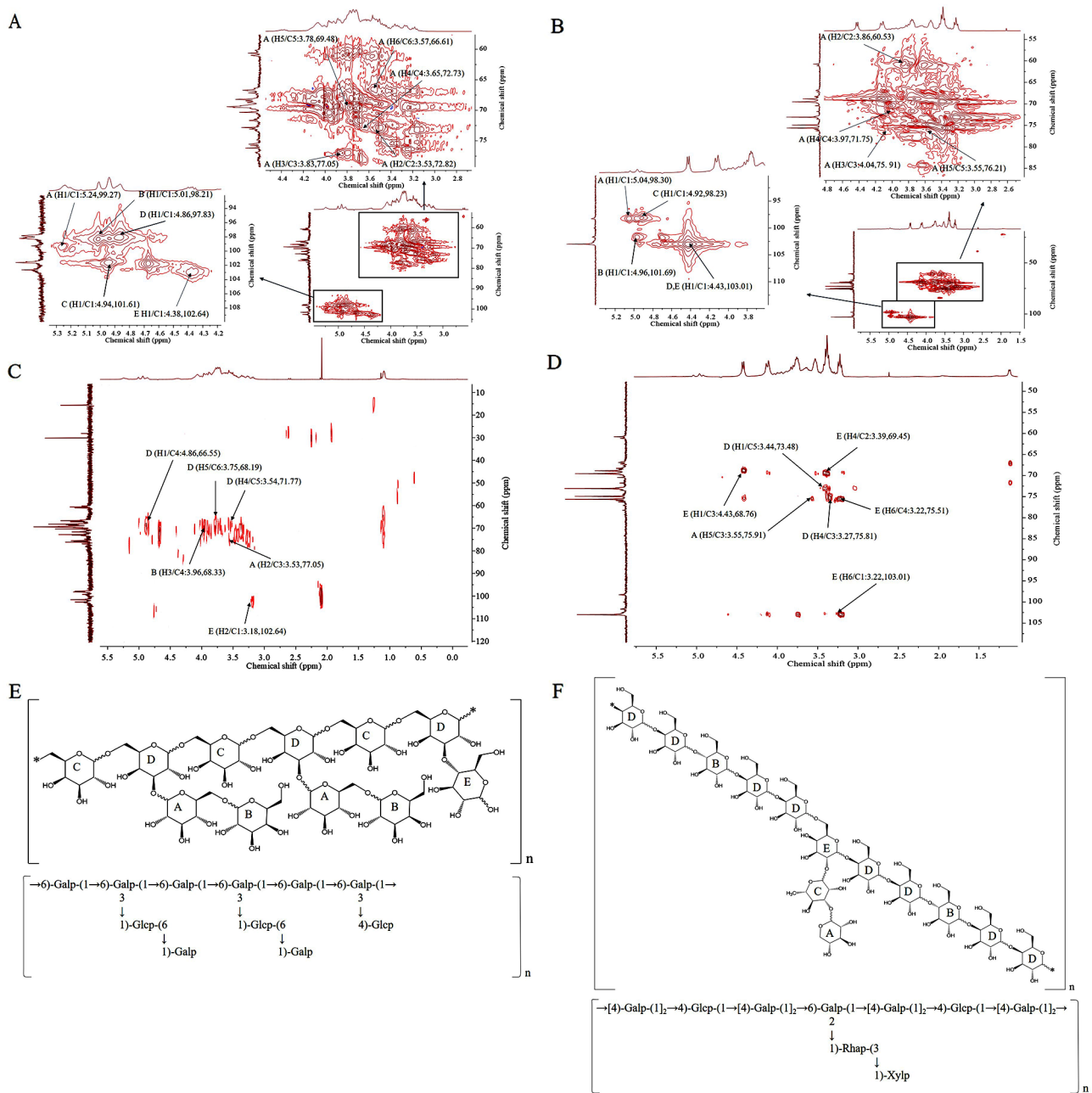
Fig. 3 **(A)** HMQC spectrum of AT-P. **(B)** HMQC spectrum of TP-P. **(C)** HMBC spectrum of AT-P. **(D)** HMBC spectrum of TP-P. **(E)** Predicted chemical structure of AT-P. **(F)** Predicted chemical structure of TP-P

of rhamnose, xylose, glucose, galactose, the ratio is 1:1:2:9, and its primary structure is based on (1→4)-galactose residue, (1→4)-glucose residue, (1→2,6)-galactose residue as the main chain, and the the branch chain were composed of (1→3)-rhamnose residue and →1)-xylose residue (Fig. 3F). The degree of branch (DB), also known as the degree of substitution (DS), also affects the activity of polysaccharides. Polysaccharides only have biological activity when they reach a certain degree of substitution. Each polysaccharide has an optimal DB to achieve its ideal biological

activity [45]. Like active polysaccharides β-(1–3)- D-glucan has strong biological activity when its branching degree is between 0.20 and 0.33. However, excessive branching can also reduce biological activity. When the branching degree of polysaccharides reaches 2.8, their biological activity is the lowest. When the branching degree of glucan is reduced to 1.0 through oxidation-reduction reaction, the anti-tumor rate almost doubles [46]. *Poria cocos* polysaccharides, due to their long-branched chains, do not exhibit biological activity and require controlled oxidative hydrolysis to

reduce the length of the branched chains to become active. In this study, AT-P was composed of glucose and galactose which had the skeleton structure consisted of $(1\rightarrow6)$-galactose residues and $(1\rightarrow3,6)$-galactose residues with three branched chains. The skeleton structure of TP-P was consisted of $(1\rightarrow4)$-galactose residues, $(1\rightarrow4)$-glucose residues and $(1\rightarrow2,6)$-galactose residues with one branched chain. The branch degree of AT-P and TP-P were 0.5 and 0.09, respectively, which indicating AT-P has better biological activity than TP-P.

Effect of AT-P and TP-P on immune cell proliferation and promotion of cytokine secretion in vitro

Polysaccharides activate immune cells including B cells, T cells, macrophages and natural killer cells to produce cytokines. The immunomodulatory effect can be used as a preventive means for metastatic tumors. T cells were a type of lymphocytes developed in the thymus and regulated the immune activity of the body [47]. The T cell proliferation efficiency increased by 38.28% and 38.73%, respectively, when the concentration of AT-P was 10 μg/mL and TP-P was 40 μg/mL (Fig. 4A and B). The morphological changes of T cells activated by AT-P and TP-P showed that the T cells grew well and the cell shape was round. The number of T cell clusters also increased, which was the same in the positive group (Fig. 4C and D).

B lymphocytes can also be abbreviated as B cells which are pluripotent stem cells and played an important role in the immune activity of the body [48]. The results showed that polysaccharide AT-P (1.25, 2.5, 5, 10, 20 μg/mL, respectively) could lead to the proliferation of B cells, and the proliferation rates was 26.33%, 26.33%, 34.54%、51.96% and 70.16%, respectively. When the concentration of AT-P was 20 μg/mL, the proliferation efficiency of B cells increased by 70.16%, and is higher than the positive control group (LPS was 10 μg/mL, 42.58%) (Fig. 5A). Compared with the blank group, the final concentration of TP-P was in the range of 10–40 μg/mL, TP-P can significantly ($P < 0.01$) promote an increase in the number of B cells, but the proliferation rate decreases with increasing concentration, with the proliferation rates being 76.28%, 71.73%, and 54.23%, respectively. Among them, when the concentration of TP-P was 10 μg/mL, its proliferation rate reached a maximum of 76.28%. (Fig. 5B). The results also showed that the B cell morphological changes in AT-P and TP-P groups (Fig. 5C and D).

Macrophages are cells differentiated from monocytes. They can participate both in the specific and the non-specific immunity of the body. Compared with the blank group, when the final concentration of AT-P was in the range of 1.25-20 μg μg/mL, AT-P could significantly increased cell proliferation rate ($P < 0.05$). When the AT-P concentration was 2.5 μg/mL, it can significantly promote the proliferation of RAW 264.7 cells ($P < 0.0001$), and the proliferation
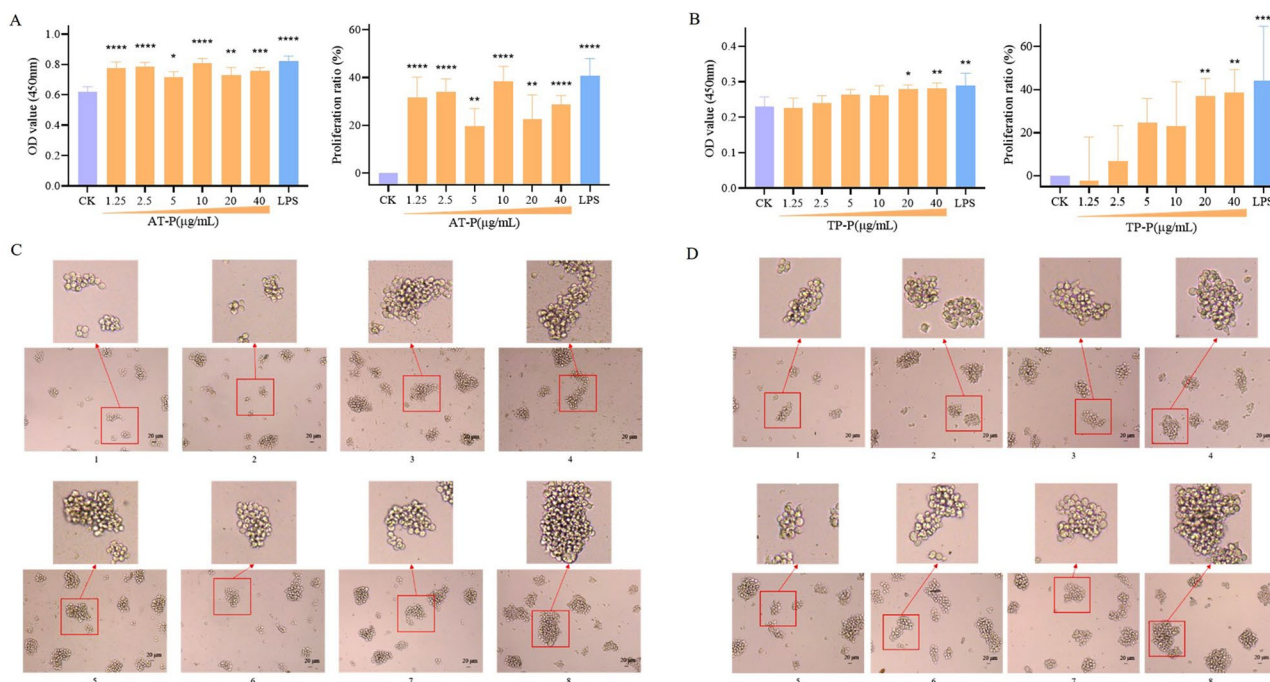
Fig. 4 **(A)** Effect on the proliferation of T cells by AT-P. **(B)** Effect on T cells morphology by AT-P. **(C)** Effect on the proliferation of T cells by TP-P. **(D)** Effect on T cells morphology by TP-P. *Note* Compared with the control group, the difference was significant ($P < 0.05$) expressed by * and very significant ($P < 0.01$) expressed by **
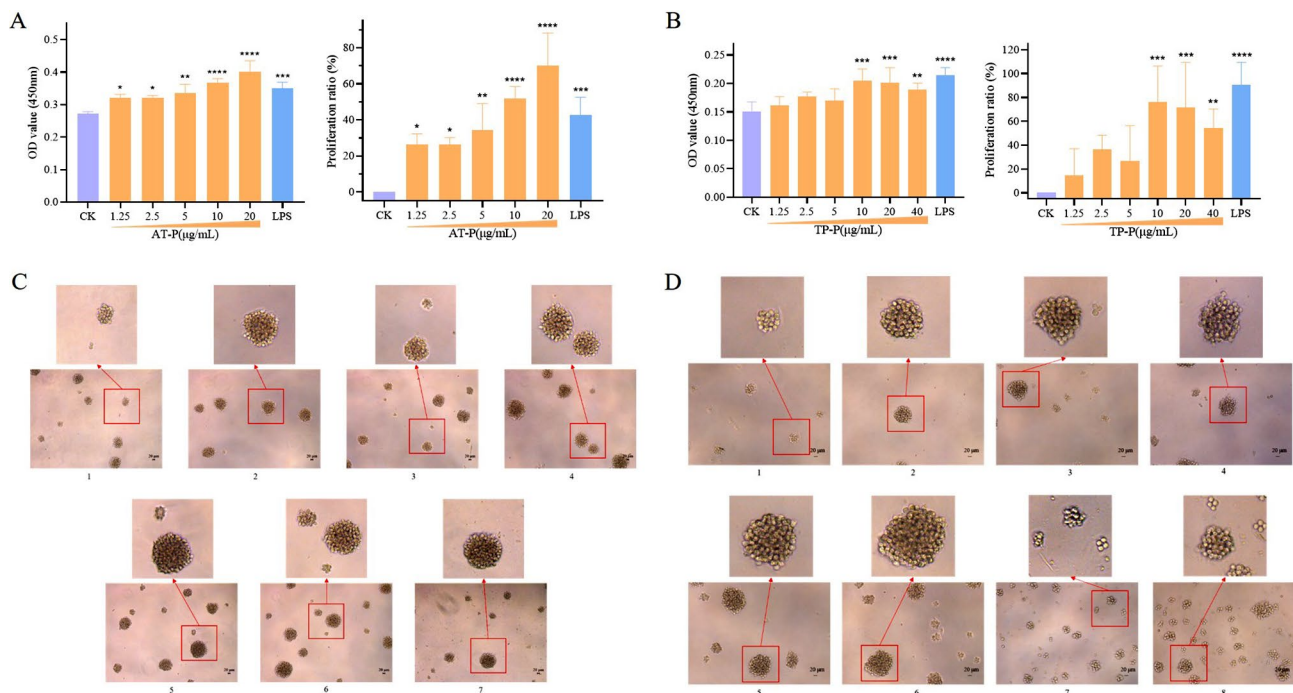
Fig. 5 (A) Effect on the proliferation of B cells by AT-P. **(B)** Effect on B cells morphology by AT-P. **(C)** Effect on the proliferation of B cells by TP-P. **(D)** Effect on B cells morphology by TP-P **(A)**. *Note* Compared with the control group, the difference was significant ($P < 0.05$) expressed by * and very significant ($P < 0.01$) expressed by **

rate reaches the highest 49.65%. Compared with the blank group, when the final concentration of TP-P was in the range of 2.5–40 µg/mL, the proliferation rate of RAW 264.7 cells was significantly increased ($P < 0.01$), with proliferation rates of 20.20%, 16.79%, 25.74%, 29.59%, and 19.12%, respectively. When the concentration of TP-P was 20 µg/mL, the proliferation efficiency of reached its maximum of 29.59% (Fig. 6A and D).

The proliferation experiment showed that the concentration of AT-P and TP-P were at 10 µg/mL and 20 µg/mL, respectively, the stimulation effect on T cells were the best, so the concentration above were selected to test their impact on the secretion of cytokine IL-10 levels in T cells. While for macrophage RAW 264.7, the concentration of 2.5 µg/mL AT-P and 20 µg/mL TP-P were selected. The experimental results showed that AT-P and TP-P had no statistically significant effects on stimulating secretion of cytokine IL-10 in T cells and RAW 264.7 cells (Fig. 7A and B).

Through cell proliferation experiments, the suitable mass concentrations of the two polysaccharides were selected to stimulate three immune cells. The experimental results indicated that TP-P can significantly ($P < 0.01$) increase the IL-1β levels of three types of immune cells in B, T, RAW 264.7 cells and the IL-1β secretion amounts was 28.73 pg/mL, 35.43 pg/mL, and 21.01 pg/mL, respectively. AT-P could significantly promote the secretion of IL-1 by B and T cells at 10 µg/mL, and it was higher than the positive control

group, reaching 38.77 pg/mL. AT-P could significantly promote the secretion of IL-1 by RAW 264.7 cells at 2.5 µg/mL. AT-P had a better effect on B cells and RAW 264.7 cells than TP-P (Fig. 7C and E).

The experimental results indicated that TP-P could significant ($P < 0.05$) increase the secretion of TNF-α by T cells and RAW 264.7 cells at 20 µg/mL and the the effect in T cells was more pronounced, with a secretion of 97.65 pg/mL. AT-P could significantly promote the secretion of TNF-α by B cells, had no significant effect on T cells, but exhibit inhibitory effect of TNF-α secretion on RAW 264.7 cells (Fig. 7F and H).

The natural immune system is the first line of defense for the body to resist the invasion of pathogenic microorganisms. The body recognizes pathogen-related molecular patterns or damage-related molecular patterns through pattern recognition receptors to initiate a natural immune response [49]. Macrophages, as one of the main cellular components in natural immunity, are considered as key immune cells for host defense, capable of clearing dead or dying cells in the body. After activation, macrophages can quickly express TNF-α, IL-6 and IL-1β cytokines, which acting as a messenger within the immune system. They could participate in the regulation of immune response by binding to specific receptors on the surface of target cells, and could also directly defend against viral infections, such as interferon, thereby mediating the body's immune response [50].
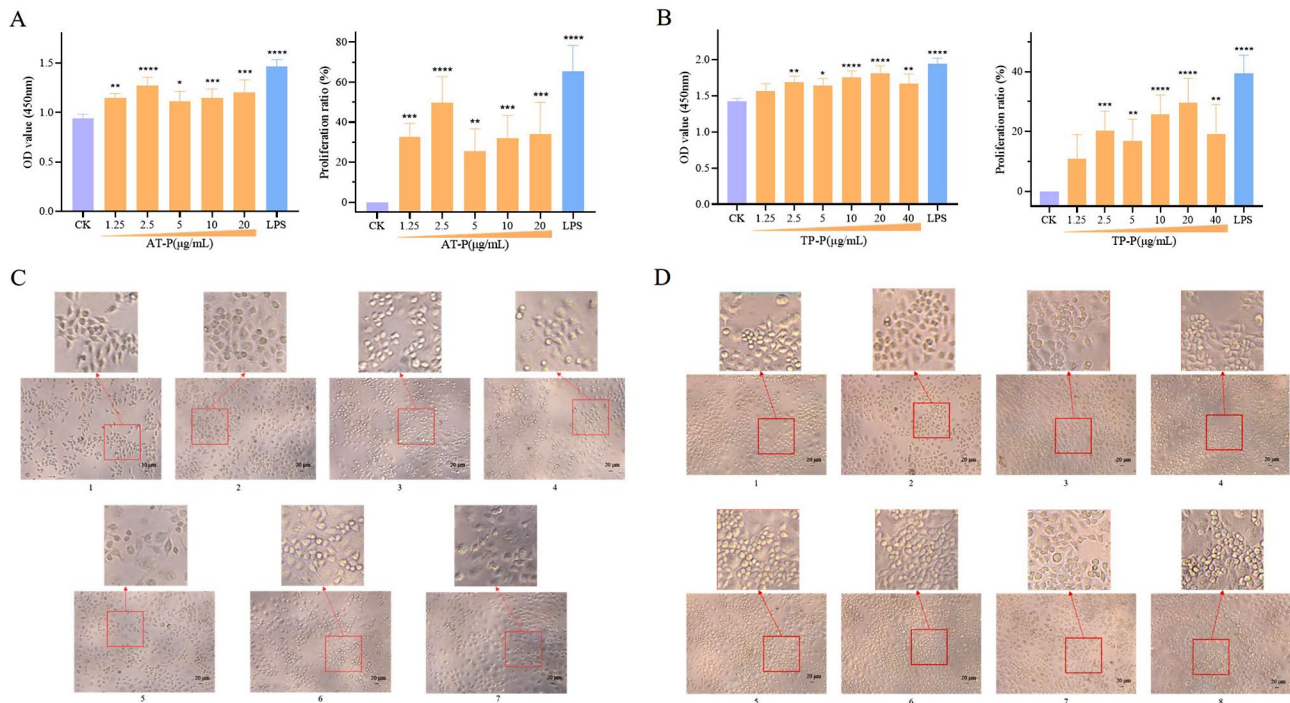
Fig. 6 **(A)** Effect on the proliferation of RAW 264.7 cells by AT-P. **(B)** Effect on RAW 264.7 cells morphology by AT-P. **(C)** Effect on the proliferation 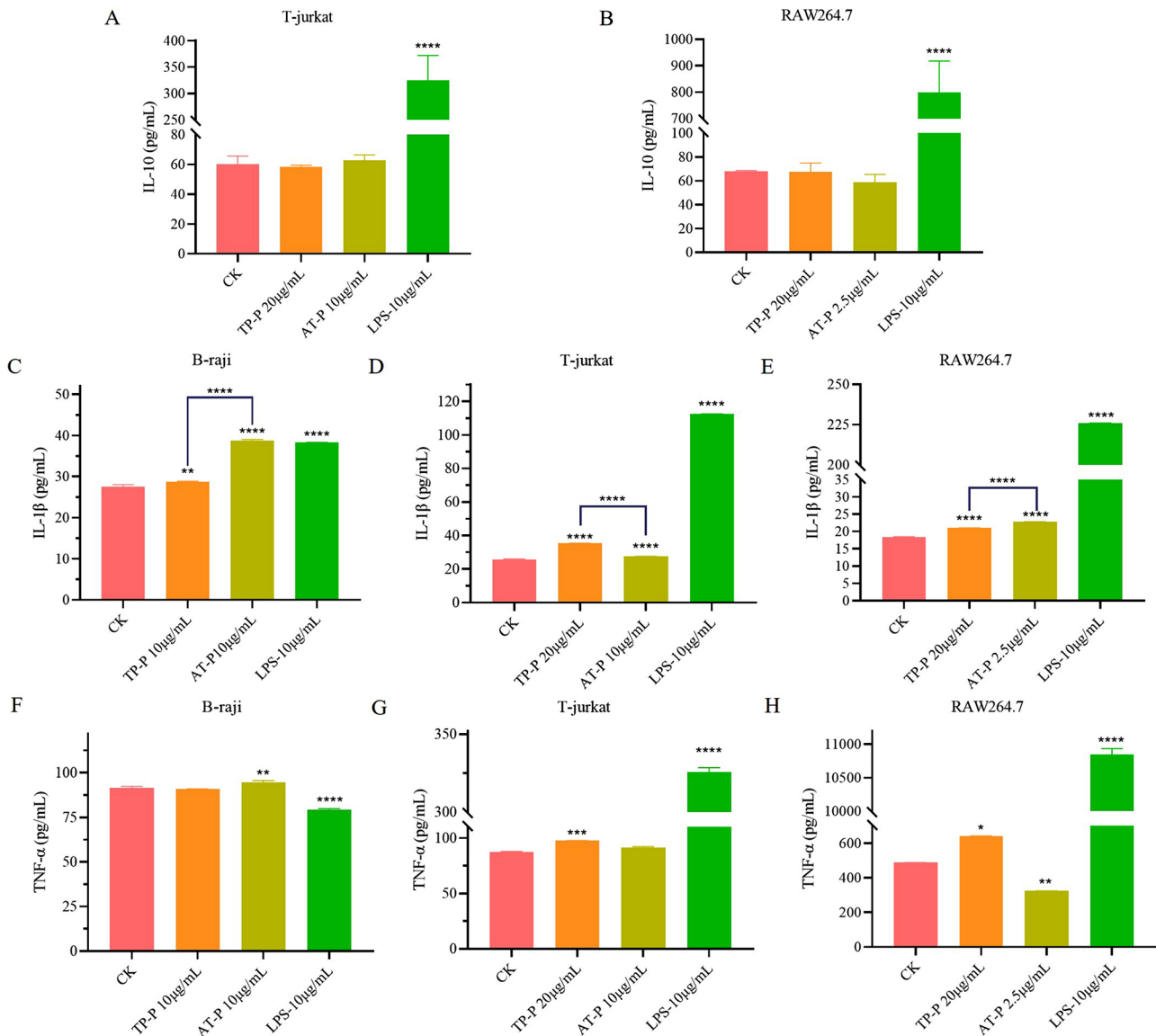of RAW 264.7 cells by TP-P. **(D)** Effect on RAW 264.7 cells morphology by TP-P. *Note* Compared with the control group, the difference was significant ($P < 0.05$) expressed by * and very significant ($P < 0.01$) expressed by **

Acquired immune response is another important component of the body's defense system, mainly played by lymphocytes to exert immune effects. Among them, B cells clear extracellular microorganisms by secreting immunoglobulins as antigen-specific antibodies, and T cells could assist B cells in producing antibodies and could also clear intracellular pathogens and viral infections by activating macrophages [51]. Polysaccharides from *Ganoderma lucidum* could induce innate inflammatory cytokines: tumor necrosis factor alpha (TNF-α), interleukin (IL) 12 and interferon gamma (IFN-γ), enhance Th1 response with high levels of IFN-γ and IL-2, and display low to no impact on IL-4 production [52]. Polysaccharides Pc-1, Pc-2, Pc-3 and Pc-4 from *Peltigera canina* had mitogenic activity in rat spleen cell proliferation and could stimulate IL-10 secretion. In rat peritoneal macrophages, these heteroglycans stimulated TNF-α secretion, but not IL-10 secretion, which indicated the polysaccharides influence cells of the immune system both from the innate and the adaptive systems [53]. Polysaccharides isolated from *Atractylodis macrocephalae* Koidz. could significantly promoted splenocyte proliferation and made the cells enter S and G2/M phases, increased ratios of T/B cells, boosted NK cytotoxicity, enhanced transcriptional activities of nuclear factor of activated T cells (NFAT) and activator protein 1 (AP-1) [54]. In this study, AT-P was suggested to have a better effect on B cells and RAW 264.7 cells than TP-P. AT-P and TP-P could significantly ($P < 0.01$)

improve the proliferation efficiency of B cells at 20 μg/mL and 10 μg/mL, respectively, with a maximum of 70.16% and 76.28%, respectively. When the AT-P and TP-P concentration was 2.5 μg/mL and 20 μg/mL, respectively, they could significantly promote the proliferation of RAW 264.7 cells ($P < 0.0001$), and the proliferation rate reaches the highest 49.65% and 29.59%, respectively. Meanwhile, AT-P was also suggested to have a better cytokines secretion effect on B cells and RAW 264.7 cells than TP-P. However, TP-P has a better cytokines secretion effect on T cells than AT-P. From the perspective of structure-activity relationship, AT-P had better branch degree, smaller molecular weight, better solubility, and was only composed of two monosaccharides, glucose and galactose. This configuration was more conducive to the formation of a three strand helical stereoconfiguration, thus exhibiting higher biological activities.

Conclusions

Polysaccharides are a class of bio-molecules commonly present in the fruiting bodies of edible and medicinal fungi. They not only participate in the composition of the cytoskeleton, but are also important components of various endogenous bioactive molecules. Polysaccharide biology, which focuses on the structure, function, and medicinal value of polysaccharides, is considered the last significant scientific

Fig. 7 **(A-B)** Effect of AT-P and TP-P on secretion of IL-10 by T cells, RAW 264.7. **(C-E)** Effect of AT-P and TP-P on secretion of IL-1β by three types of immune cells. **(F-H)** Effect of AT-P and TP-P on secre- tion of TNF-α by three types of immune cells. *Note* Compared with the control group, the difference was significant ($P < 0.05$) expressed by * and very significant ($P < 0.01$) expressed by **

frontier in the field of protein and nucleic acid research. But because of their complex composition, large molecular weight, difficulty of purification and complicated structure, not many kinds of them had been approved as drugs by the national authority. There are currently 7 types of approved polysaccharide drugs in China, including *Radix Astragali seu Hedysari* polysaccharide, *Ganoderma* polysaccharide, *Poria* polysaccharide, *Radix Ginseng* polysaccharide, etc. These polysaccharide drugs are mostly used to regulate immunity, but their mechanisms of action are complex. Further understanding the composition and structure of active polysaccharides from edible and medicinal fungi, elucidating their molecular mechanisms for activating and

regulating immune cells, has guiding significance for the development of active polysaccharides from edible and medicinal fungi. In this study, the structure characterization of two new polysaccharides from *Armillariella tabescens* (AT-P) and *Tricholoma portentosum* (TP-P) by HPGPC, GC-MS, NMR and FT-IR indicated that AT-P was com- posed of glucose and galactose in a ratio of 3:8. Its skeleton structure was consisted of (1→6)-galactose residues and (1→3,6)-galactose residues with three branched chains. The TP-P was consisted of composed of rhamnose, xylose, glu- cose, galactose in the ratio of 1:1:2:9. Its skeleton structure was consisted of (1→4)-galactose residues, (1→4)-glucose residues and (1→2,6)-galactose residues with one branched

chain. Within the concentration range of 1.25 and 40 µg/mL, both AT-P and TP-P could enhance the proliferation ability of T cells, B cells, and RAW 264.7 cells. AT-P and TP-P could significantly ($P < 0.01$) improve the proliferation efficiency of B cells at 20 µg/mL and 10 µg/mL, respectively, with a maximum of 70.16% and 76.28%, respectively. Both AT-P and TP-P could promote the secretion of IL-1β and TNF-α by RAW 264.7 cells and promote the secretion of IL-1 by B and T cells. However, neither of they could not promote the secretion of IL-10 by RAW 264.7 cells and T cells. Their effects on the secretion of TNF-α by T and B cells were also different. Our research indicated that the monosaccharide composition, monosaccharide linkage, molecular weight, branch degree, solubility and functional groups of polysaccharides all played a certain impact on their biological activity. The biological activity of polysaccharides is a comprehensive effect generated by the mutual constraints between various levels of structure, structure and physicochemical properties, and various physicochemical properties. Currently, there is still insufficient research on the structure and structure-activity relationship of polysaccharides. With the improvement of separation and structural identification methods, as well as the deepening of polysaccharide research, active polysaccharides will continue to be developed into new drugs, and their clinical applications and the scale will continue to expand.

Declarations

Conflict of interest The authors declare that they have no competing interests.

Research involving human and animal participants The manuscript does not contain experiments using animals or human studies.

References

1. S. Su, X. Ding, Y. Hou, B. Liu, Z. Du, J. Liu, Food Sci. Hum. Wellness. **12**(2), 647–661 (2023). https://doi.org/10.1016/j.fshw.2022.07.067
2. G.A. Rougon, J. Cell. Bio. **103**(6), 2429–2437 (1986). https://doi.org/10.2307/1612193
3. I. Wijesekara, R. Pangestuti, S.K. Kim, Carbohydr. Polym. **84**(1), 14–21 (2011). https://doi.org/10.1016/j.carbpol.2010.10.06
4. G.P.C. Filho, A.F.G. Sousa, R.B.G. Câmara, H.A.O. Rocha, S.R.B. Medeiros, S. Moreira, Int. J. Biol. Macro. **114**, 565–571 (2018). https://doi.org/10.1016/j.ijbiomac.2018.03.132
5. M. Kozarski, A. Klaus, M. Niksic, D. Jakovljevic, J.P. Helsper, L.J. Van Griensven, Food Chem. **129**(4), 1667–1675 (2011). https://doi.org/10.1016/j.foodchem.2011.06.029
6. K. Kouakou, I.A. Schepetkin, A. Yapi, L.N. Kirpotina, M.T. Quinn, J. Ethnopharm. **146**(1), 232–242 (2013). https://doi.org/10.1016/j.jep.2012.12.037
7. R. Sullivan, J.E. Smith, N.J. Rowan, Int. J. Med. Mushrooms. **5**(2), 16–16 (2003). https://doi.org/10.1615/InterJMedicMush.v5.i2.10
8. A.B. Samuelsen, A. Rieder, S. Grimmer, T.E. Michaelsen, S.H. Knutsen, Int. J. Mol. Sci. **12**(1), 570–587 (2011). https://doi.org/10.3390/ijms12010570
9. S.C. Sheu, L. Ying, M.S. Lee, J.H. Cheng, Process. Biochem. **48**(9), 1402–1408 (2013). https://doi.org/10.1016/j.procbio.2013.06.012
10. N.J. Horan, C.R. Eccles, Water Res. **20**(11), 1427–1432 (1986). https://doi.org/10.1016/0043-1354(86)90142-9
11. M.A. Coimbra, M. Barros, A. Barros, D. Rutdledge, I. Delgadillo, Carbohydr. Polym. **34**(4), 426–426 (1997). https://doi.org/10.1016/S0144-8617(97)87351-1
12. A.J.A. Charlton, A. Jones, J. Chromatogr. A **1141**(1), 117–122 (2007). https://doi.org/10.1016/j.chroma.2006.11.107
13. J.H. Xie, M.Y. Xie, S.P. Nie, M.Y. Shen, Y.X. Wang, C. Li, Food Chem. **119**(4), 1626–1632 (2010). https://doi.org/10.1016/j.foodchem.2009.09.055
14. A. Scamparini, D. Mariuzzo, H. Fujihara, R. Jacobusi, C. Vendruscolo, Int. J. Biol. Macro **21**(1–2), 115–121(1997). https://doi.org/10.1016/S0141-8130(97)00050-0
15. K.J. Jeon, K. Katsuraya, Y. Kaneko, T. Mimura, T Uryu FIBER. **53**(12), 533–539 (2008). https://doi.org/10.2115/fiber.53.12_533
16. M. Zeng, Q. Kong, F. Liu, J. Chen, H. Sang, Inter. J. Polym. Sci. 2019, 1–8(2019). https://doi.org/10.1155/2019/5065920
17. J. Li, Y. Cui, Q. Wang, D. Guo, S. Zhao, Mol. Vis. **20**(236), 649–660 (2014). https://doi.org/10.1186/2241-5793-21-5
18. H. Xu, Q. Zhou, B. Liu, F. Cheng, M. Wang, Carbohydr. Polym. **275**, 118691 (2024). https://doi.org/10.1016/j.carbpol.2021.118691
19. V.N. Reinhold, B.B. Reinhold, C.E. Costello, Anal. Chem. **67**(11), 1772–1784 (1995). https://doi.org/10.1021/ac00107a005
20. H. Amekura, N. Umeda, N. Okubo, N. Kishimoto, Nuclear Inst & Methods in Physics Research B, 206, 1101–1105 (2003). https://doi.org/10.1016/S0168-583X(03)00919-4
21. M.C. Zoerb, J.S. Henderson, S.D. Glover, J.P. Lomont, S.C. Nguyen, A.D. Hill et al., J. Phys. Chem. B **119**(33), 10738–10749 (2015). https://doi.org/10.1021/acs.jpcb.5b06734
22. M. Cerná, S.B. António, A. Nunes, S.M. Rocha, M.A. Coimbra, Carbohydr. Polym. **51**(4), 383–389 (2003). https://doi.org/10.1016/S0144-8617(02)00259-X
23. K. Tadashi, S. Yoshinobu, N. Katsuyuki, S. Miho, U. Shigeo, Chem. Pharm. Bull. (Tokyo). **40**(8), 2212–2214 (1992)
24. X. Chen, T. Yang, Q. Huang, B. Li, X. Ding, Y. Hou, Polymers. **15**, 2227–2246 (2023). https://doi.org/10.3390/polym15092227
25. A.B. Samuelsen, I. Lund, J. Djahromi, B.S. Paulsen, S. Knutsen, Carbohydr. Polym. **38**(2), 133–143 (1999). https://doi.org/10.1016/S0144-8617(98)00115-5
26. S.P. Nie, C. Wang, S.W. Cui, Q. Wang, M.Y. Xie, G.O. Phillips, Food Hydrocoll. **31**(1), 42–48 (2013). https://doi.org/10.1016/j.foodhyd.2012.09.014
27. H. Kiyohara, M. Hirano, X.G. Wen, T. Matsumoto, X.B. Sun, H. Yamada, Carbohydr. Res. **263**(1), 89–101 (1994). https://doi.org/10.1016/0008-6215(94)00151-0
28. P.C. Wang, S. Zhao, B.Y. Yang, Q.H. Wang, H.X. Kuang, Carbohydr. Polym. **148**, 86–97 (2016). https://doi.org/10.1016/j.carbpol.2016.02.060
29. X. Ji, J. Guo, T. Cao, T. Zhang, Y. Liu, Y. Yan, Food Sci. Hum. Wellness. **12**(6), 1969–1980 (2023). https://doi.org/10.1016/j.fshw.2023.03.017
30. C. Fontana, G. Widmalm, Chem. Rev. **123**, 1040–1102 (2023). https://doi.org/10.1021/acs.chemrev.2c00580

31. P. Strunk, T. Oeman, A. Gorzsas, M. Hedenstroem, B. Eliasson, Nordic Pulp Paper Res. J. **26**(4), 398–409 (2011). https://doi.org/10.4067/S0718-221X2011000300010

32. K. Higashi, M. Ly, Z. Wang, S. Masuko, U. Bhaskar, E. Sterner et al., Carbohydr. Polym. **86**(3), 1365–1370 (2011). https://doi.org/10.1016/j.carbpol.2011.06.042

33. K.R. Morgan, J.A. Hemmingson, R.H. Furneaux, R.A. Stanley, Carbohydr. Res. **262**(2), 185–194 (1994). https://doi.org/10.1016/0008-6215(94)84178-0

34. L. Pereira, A. Sousa, H. Coelho, A.M. Amado, P.J. Ribeiro-Claro, Biomol. Eng. **20**(4–6), 223–228 (2003). https://doi.org/10.1016/S1389-0344(03)00058-3

35. Y. Tamaki, S. Uechi, T. Taira, M. Ishihara, S. Adaniya, K. Uesato, J. Appl. Glycoscience. **51**(1), 19–25 (2008). https://doi.org/10.5458/jag.51.19

36. N.E. Schlrer, E.J. Cabrita, S. Berger, Angew. Chem. Int. Ed. **41**(1), 107–109 (2002). https://doi.org/10.1002/1521-3773(20020104)41:13.0.CO;2-N

37. K. Yamashita, K. Yamamoto, J.I. Kadokawa, Biomacromolecules. **16**(12), 3989 (2015). https://doi.org/10.1021/acs.biomac.5b01332

38. M. Urai, H. Yoshizaki, H. Anzai, J. Ogihara, N. Iwabuchi, S. Harayama et al., Carbohydr. Res. **342**(7), 927–932 (2007). https://doi.org/10.1016/j.carres.2007.02.002

39. H. Kim, J. Ralph, Bioenergy Res. **8**(3), 576–591 (2010). https://doi.org/10.1039/b916070a

40. R. Sarkar, C.K. Nandan, S.K. Bhunia, S. Maiti, T.K. Maiti, S.R. Sikdar et al., Carbohydr. Res. **347**(1), 107–113 (2012). https://doi.org/10.1016/j.carres.2011.10.043

41. V.H. Pomin, V.A. Paula, M.S. Pereira, A.S. Mourão, Paulo Glycobiology. **12**, 1376–1385 (2005). https://doi.org/10.1016/j.synthmet.2007.10.003

42. T.D.W. Claridge, I. Pérez-Victoria, Org. Biomol. Chem. **1**(21), 3632–3634 (2003). https://doi.org/10.1039/b307122g

43. A.N. Kondakova, F.V. Toukach, S.N. Senchenkova, N.P. Arbatsky, A.S. Shashkov, Y.A. Knirel et al., Biochemistry. **67**(2), 201–211 (2002). https://doi.org/10.1023/a:1014414030784

44. A. Omaira, P.G. León de, M. Maritza, G. Omaira, S. Lilian, Food Hydrocoll. **21**(8), 1302–1309 (2007). https://doi.org/10.1016/j.foodhyd.2006.10.004

45. D.S. Tolmasky, C.R. Krisman, Eur. J. Biochem. **168**(2), 393–397 (2005). https://doi.org/10.1111/j.1432-1033.1987.tb13432.x

46. A. Pawlowski, G. Kllenius, S.B. Svenson, Vaccine. **17**(11–12), 1474–1483 (1999). https://doi.org/10.1016/S0264-410X(98)00385-5

47. H. Park, L. Zhaoxia, Y. Xuexian, O. Seon, H. Chang, Nat. Immu. **6**(11), 1133–1141 (2005). https://doi.org/10.1038/ni1261

48. K.I. Lin, C. Angelin-Duclos, T.C. Kuo, K. Calame, Mol. Cell. Bio. **22**, 4771–4780 (2002). https://doi.org/10.1128/mcb.22.13.4771-4780.2002

49. C.J. Binder, P.X. Shaw, M.K. Chang, A. Boullier, J.L. Witztum, J. Lipid Res. **46**(7), 1353–1363 (2005). https://doi.org/10.1194/jlr.R500005-JLR200

50. A. Mantovani, S. Sozzani, P. Allavena, M. Locati, A. Sica, Trends Immunol. **23**(11), 549–555 (2002). https://doi.org/10.1016/S1471-4906(02)02302-5

51. Y. Benhamou, N. Kapel, C. Hoang, H. Matta, D. Meillet, D. Magne et al., Gastroenterology. **108**(3), 627–635 (1995). https://doi.org/10.1016/0016-5085(95)90433-6

52. J. Habijanic, M. Berovic, B. Boh, M. Plankl, B. Wraber, New. Biotech. **32**(1), 85–95 (2015). https://doi.org/10.1016/j.nbt.2014.07.007

53. S. Omarsdottir, J. Freysdottir, H. Barsett, B.S. Paulsen, E.S. Olafsdottir, Phytomedicine Inter J. Phytotherapy Phytopharmacology. **12**(6–7), 461–467 (2005). https://doi.org/10.1016/j.phymed.2004.03.012

54. W. Xu, S. Fang, X. Cui, R. Guan, Y. Wang, F. Shi et al., Mol. Immuno. **111**, 19–26 (2019). https://doi.org/10.1016/j.molimm.2019.03.004